0022-3565/09/3293-978–986$20.00
THE JOURNAL OF PHARMACOLOGY AND EXPERIMENTAL THERAPEUTICS
JPET 329:978–986, 2009

Vol. 329, No. 3
146175/3477423
Printed in U.S.A.

Compartmentalized β Subunit Distribution Determines Characteristics and Ethanol Sensitivity of Somatic, Dendritic, and Terminal Large-Conductance Calcium-Activated Potassium Channels in the Rat Central Nervous System

P. M. Wynne, S. I. Puig, G. E. Martin, and S. N. Treistman[1]

Brudnick Neuropsychiatric Research Institute, University of Massachusetts Medical School, Worcester, Massachusetts

Received October 17, 2008; accepted March 24, 2009

ABSTRACT

Neurons are highly differentiated and polarized cells, whose various functions depend upon the compartmentalization of ion channels. The rat hypothalamic-neurohypophysial system (HNS), in which cell bodies and dendrites reside in the hypothalamus, physically separated from their nerve terminals in the neurohypophysis, provides a particularly powerful preparation in which to study the distribution and regional properties of ion channel proteins. Using electrophysiological and immunohistochemical techniques, we characterized the large-conductance calcium-activated potassium (BK) channel in each of the three primary compartments (soma, dendrite, and terminal) of HNS neurons. We found that dendritic BK channels, in common with somatic channels but in contrast to nerve terminal channels, are insensitive to iberiotoxin. Furthermore, analysis of dendritic BK channel gating kinetics indicates that they, like somatic channels, have fast activation kinetics, in contrast to the slow gating of terminal channels. Dendritic and somatic channels are also more sensitive to calcium and have a greater conductance than terminal channels. Finally, although terminal BK channels are highly potentiated by ethanol, somatic and dendritic channels are insensitive to the drug. The biophysical and pharmacological properties of somatic and dendritic versus nerve terminal channels are consistent with the characteristics of exogenously expressed $\alpha\beta1$ versus $\alpha\beta4$ channels, respectively. Therefore, one possible explanation for our findings is a selective distribution of auxiliary $\beta1$ subunits to the somatic and dendritic compartments and $\beta4$ to the terminal compartment. This hypothesis is supported immunohistochemically by the appearance of distinct punctate $\beta1$ or $\beta4$ channel clusters in the membrane of somatic and dendritic or nerve terminal compartments, respectively.

Ion channel compartmentalization between specific brain regions and various neuronal populations has been known for many years. Technological advances recently have permitted researchers to probe the distribution of channel subtypes on a subcellular level. Here, we have utilized a unique system, the hypothalamic-neurohypophysial system (HNS), which allows us to examine dendrites, cell bodies, and individual nerve terminals within the same population of magnocellular neurons. The HNS is an ideal model system to study compartmentalization of channel properties because the three neuronal domains (dendrite, cell body, and nerve terminal) can be easily distinguished from one another. The large (20–30 μm) magnocellular neurons of the supraoptic nucleus (SON) send axonal projections to the posterior pituitary (neurohypophysis), where they terminate in thousands of nerve endings that release oxytocin (OXT) or vasopressin (AVP) into systemic circulation. Magnocellular neuron dendrites, on the other hand, project toward the ventral surface of the brain, forming a dense interlaced network that releases OXT or AVP centrally. HNS axons morphologically have few, if any, collaterals, allowing them to be easily distinguished from dendrites.

Large-conductance calcium-activated potassium (BK) channels play a prominent role in cellular excitability from repolarizing neuronal action potentials to modulating contractility in vasculature. They are found ubiquitously throughout the brain and are highly conserved in mammals. BK channels are activated by both cell membrane depolarization and increases in intracellular calcium, allowing them

This work was supported by the National Institutes of Health National Institute on Alcohol Abuse and Alcoholism [Grants 1F31-AA01547401A1, 5RO1-AA0800318, R37-AA1205403].

[1]Current affiliation: University of Puerto Rico, Institute of Neurobiology, San Juan, Puerto Rico.

Article, publication date, and citation information can be found at http://jpet.aspetjournals.org.
doi:10.1124/jpet.108.146175.

ABBREVIATIONS: HNS, hypothalamic-neurohypophysial system; SON, supraoptic nucleus; OXT, oxytocin; AVP, vasopressin; BK, large-conductance calcium-activated potassium; HEDTA, *N*-hydroxy-EDTA; PBS, phosphate-buffered saline; EtOH, ethanol; IbTX, iberiotoxin; NMDA, *N*-methyl-D-aspartate; NP_o, channel open probability.

to function as coincidence detectors that integrate intracellular calcium levels and membrane voltage. BK channels may be homomeric or heteromeric and are composed of four seven-transmembrane α subunits that form the selectivity pore of the channel.

Currently, four β subunits (β1–β4) have been cloned and characterized. Association of the α subunit with various β subunits modulates channel properties, including kinetic behavior, voltage dependence, calcium sensitivity, and pharmacological attributes such as sensitivity to the channel blockers, iberiotoxin and charybdotoxin (Dworetzky et al., 1996; Lippiat et al., 2003). To date, studies examining the regional distribution of BK β subunits indicate that they are relatively tissue specific. Several studies indicate that β1 subunits are localized primarily in smooth muscle, showing less expression in the brain (Jiang et al., 1999). β2 Subunit expression is especially abundant in ovaries, whereas β3 shows the highest expression in the pancreas and testis. The β2 and β3 subunits are only weakly detected in other tissues, including brain (Wallner et al., 1996; Brenner et al., 2000). In contrast to the other β subunits, β4 is highly expressed in brain and only weakly detected in other tissues (Brenner et al., 2000).

On the subcellular level, few studies have attempted to describe BK channel distribution, characterization, and subunit composition in all three compartments of a neuron. Studies have described the immunolocalization of BK channels in the dendrites and nerve terminals of hippocampal pyramidal neurons but did not biophysically characterize or identify the subunit composition of the channels (Sailer et al., 2006). In another example, Benhassine and Berger (2005) determined that the biophysical properties of dendritic and somatic BK channels in layer 5 pyramidal neurons of the somatosensory cortex were identical but did not examine channels in nerve terminals. We have reported previously that dendritic and somatic BK channels in rat nucleus accumbens neurons display different biophysical properties, which could be explained by a predominance of BK β1 subunits in the dendritic compartment and BK β4 subunits in the cell body (Martin et al., 2004). Again, because of limitations of the preparation, this study was unable to examine BK channels in nucleus accumbens nerve terminals. Here, we focus on BK channels within HNS magnocellular neurons and describe the characteristics of BK channels in each of the three major compartments of a central nervous system neuron. These findings may have functional significance in understanding how peptide release from the dendritic, somatic, and nerve terminal compartment is differentially regulated (for review, see Ludwig and Leng, 2006).

Materials and Methods

Isolated SON Cell Bodies. Adult Sprague-Dawley rats (150–250 g) were decapitated, and the brain was removed and placed into a dish containing oxygenated ice-cold (4°C) high-sucrose cutting solution. Slices (500 μm) were obtained using a Vibroslicer, and the SON was isolated with the aid of a dissecting microscope and transferred to an oxygenated (100% O_2 with constant stirring) Hanks' balanced salt solution containing Protease XIV from *Streptomyces griseus* (Sigma-Aldrich, St. Louis, MO) for 15 min. The SON disks were then transferred to Earle's balanced salt solution (holding) solution oxygenated with 95% O_2/5% CO_2 for 45 min. The tissue was then mechanically triturated in sodium isethionate solution using fire-polished Pasteur pipettes with successively smaller tip diameters. Dissociated cell bodies were then transferred to a 35-mm Petri dish placed on the stage of an inverted microscope (Nikon Diaphot; Nikon, Tokyo, Japan). The cells were allowed to settle for 15 min before perfusing with 60 ml of regular Locke's solution at a rate of 4 ml/min. Electrophysiological recordings were subsequently obtained from either the cell body or dendrite. In contrast to axons, which have a uniform width and lack any branches, dendrites were identified morphologically by their tapered appearance and branching (Fig. 1A).

Isolated Neurohypophysial Terminals. The neurohypophysis was removed from the animal within 1 min of sacrifice and placed in low-calcium Locke's solution. To expose the neurohypophysis, the pars intermedia was dissected away and discarded. Terminals were homogenized in a solution containing 270 mM sucrose, 10 mM HEPES, and 1 mM EGTA, pH 7.3, and transferred to a 35-mm dish, where they were allowed to settle. The terminals were then processed for immunohistochemistry or electrophysiology. For electrophysiological measurements, dissociated terminals were identified by their spherical shape, approximately 6-μm diameter, lack of nuclei, and golden color under Hoffman phase-contrast optics. Before ethanol challenge, the terminals were first bathed in low-calcium (3 μM free Ca^{2+}) Locke's solution followed by regular Locke's solution.

Single-Channel Recordings. Recording electrodes were pulled (Sutter Instrument Company, Novato, CA) and fire-polished from borosilicate capillary glass (Drummond Scientific, Broomall, PA) to a final resistance of 4 to 8 MΩ. Currents were recorded in voltage-clamp mode with a HEKA EPC 10 amplifier at a sampling rate of 10 kHz and low-pass filtered at 2.0 kHz with an eight-pole Bessel filter. Potentials and currents were digitized, curve-fit, measured, stored,

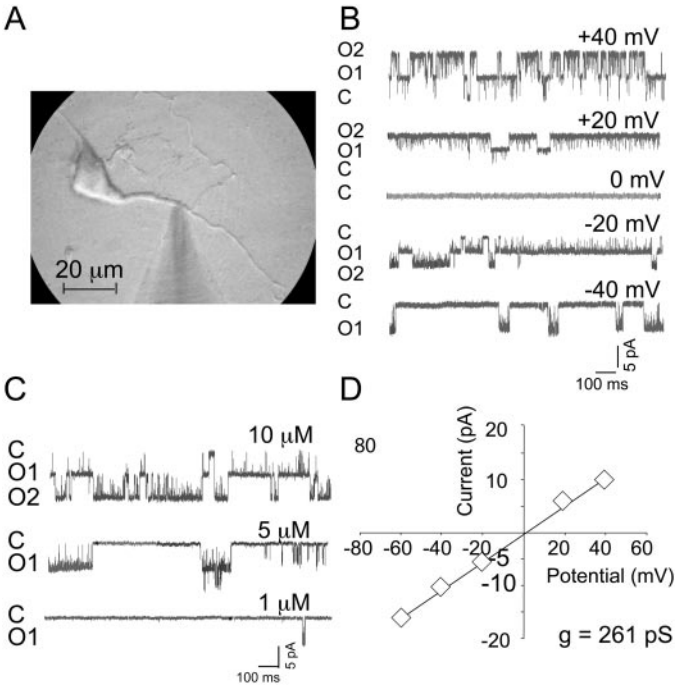

Fig. 1. Voltage and calcium dependence of dendritic BK channels of HNS magnocellular neurons. A, micrograph of a recording electrode positioned on the dendrite of a dissociated SON neuron. B, time spent in the open state by two dendritic BK channels, recorded in inside-out patch-clamp configuration in the presence of 5 μM free Ca^{2+}, increases as the membrane is depolarized. C, traces recorded at −40 mV in the same patch as in B show the dependence of channel activity on intracellular calcium (1–10 μM). D, plot of BK channel current amplitude as a function of membrane potential calculated from results in B. A linear fit of this relationship ($r = 0.99$) gave a BK channel unitary conductance of 261 pS. C and O, closed and open states, respectively. The number next to the letter O represents the number of channel(s) simultaneously open.

and plotted using Patchmaster acquisition and analysis software (HEKA, Lambrecht/Pfalz, Germany).

Data Analysis. NP_o values were calculated from all-points amplitude histograms by fitting the histogram with a sum of Gaussian functions using a Levenberg-Marquardt algorithm. NP_o data as a function of voltage were fitted with a Boltzmann function of the type: $P_o = (1 + \exp - K(V - V_{0.5}))^{-1}$, where K is the logarithmic potential sensitivity, and $V_{0.5}$ the potential at which P_o is half-maximal. When the NP_o-voltage relationship is fitted by a Boltzmann curve, a plot of $\ln NP_o$ versus voltage is linear at low values of P_o. In this plot, the reciprocal of the slope is the potential needed to produce an e-fold change in NP_o, which is routinely used to measure the voltage dependence of BK channel gating. The unitary conductance (γ) was taken as the slope of the unitary current amplitude-voltage relationship. Values for unitary current were obtained from the Gaussian fit of all-points amplitude histograms by measuring the distance between the modes corresponding to the closed state and the first opening level. In single-channel patches, durations of open and closed times were measured with half-amplitude threshold analysis. A maximal likelihood minimization routine was used to fit curves to the distribution of open or closed times. For all experiments, voltages given correspond to the potential at the intracellular side of the membrane.

Macroscopic currents were compiled by summing 100 consecutive single-channel traces obtained by stepping the membrane of an inside-out patch from a holding potential of 0 to +40 mV, in the presence of 10 μM free Ca^{2+}. Leak currents were subtracted on-line. To yield the macroscopic current, traces were summed and the activation kinetics subsequently fit using Fitmaster software (HEKA).

Ethanol and Iberiotoxin Application. Recording electrode tips were positioned in the "mouth" of the perfusion pipe (hematocrit tubes) to prevent contamination from solutions potentially leaking from nearby tubes. Three 20-s control traces in the presence of 5 μM free Ca^{2+} solution were taken to determine baseline channel activity. Ethanol or iberiotoxin were applied to inside-out or outside-out patches, respectively.

Experimental Solutions. High-potassium pipette solution contained 135 mM potassium gluconate, 1 mM $MgCl_2$, 2.2 mM $CaCl_2$, 15 mM HEPES, 4 mM EGTA, and 4 mM HEDTA. Regular Locke's solution contained 2 mM KCl, 142 mM NaCl, 2 mM $MgCl_2$, 2 mM $CaCl_2$, 13 mM glucose, and 15 mM HEPES. During all recording sessions, excised patches were exposed to 135 to 140 mM potassium gluconate, 0 to 4 mM HEDTA, 0 to 4 mM EGTA, 15 mM HEPES, 1 mM $MgCl_2$, and 0.5 to 2.2 mM $CaCl_2$. HEDTA, EGTA, and $CaCl_2$ concentrations were adjusted to obtain the desired concentrations of free calcium, ranging from 1 to 25 μM. Free Ca^{2+} concentrations were determined by the Max Chelator Sliders software (C. Patton, Stanford University, Palo Alto, CA) and confirmed with a Kwik-Tip calcium probe (World Precision Instruments, Inc., Sarasota, FL). In these conditions, K^+ concentrations on either side of membrane patches were the same in all experiments. Regular Locke's solution was used to wash the recording chamber only.

Immunohistochemistry. To stain the SON, a block of brain tissue was fixed in 4% paraformaldehyde. After immersion in 20% sucrose, tissue was embedded in 6% gelatin-egg yolk mixture and exposed to concentrated formaldehyde vapors for at least 3 days (4°C). After hardening, 50 μM coronal sections were cut on a freezing microtome, placed in 1× PBS, and transferred to wells. HNS terminals were dissociated, as described previously, allowed to settle for 15 min on glass bottom culture dishes (MatTek, Ashland, MA), and fixed in 4% paraformaldehyde. Both the terminals and SON tissues slices were then permeabilized and blocked in a solution containing 10% normal goat serum, 0.1% bovine serum albumin, and 0.4% Triton X-100 in PBS/0.02% sodium azide, pH 7.4, for 1 h at room temperature.

Permeabilized SON sections were incubated with primary antibodies to polyclonal anti-BK β1 (1:100; Alomone Labs, Jerusalem, Israel) or polyclonal anti-BK β4 subunit (1:100; Alomone Labs) overnight at 4°C. After incubation, SON slices were rinsed and incubated for 1 h at room temperature with Alexa 488-tagged anti-rabbit secondary antibody (1:300; Invitrogen, Carlsbad, CA) for 1 h at room temperature. After rinsing, SON sections were incubated with goat anti-vasopressin (1:100; Santa Cruz Biotechnology, Inc., Santa Cruz, CA) for 2 h at room temperature, rinsed, and incubated with Alexa 594-tagged anti-goat secondary antibody. After ample washing with PBS, SON tissue slices were mounted on microslides (SuperFrost Plus; VWR, West Chester, PA) using Prolong Antifade medium (Invitrogen, Carlsbad, CA).

Permeabilized nerve terminals were incubated with primary antibodies to polyclonal anti-BK β1 (1:100; Alomone Labs) or polyclonal anti-BK β4 subunit (1:100; Alomone Labs) overnight at 4°C. After incubation, terminals were rinsed and incubated for 1 h at room temperature with Alexa 594-tagged anti-rabbit secondary antibody (1:300; Molecular Probes) for 1 h at room temperature. After rinsing, terminals were incubated with goat anti-vasopressin (1:100; Santa Cruz Biotechnology, Inc.) for 2 h at room temperature, rinsed, and incubated with Alexa 350-tagged anti-goat secondary antibody. After rinsing, terminals were incubated with mouse anti-oxytocin (1:100, a gift from Dr. H. Gainer) for 2 h at room temperature, rinsed, and incubated with Alexa 488-tagged anti-mouse secondary antibody for 1 h at room temperature. Coverslips were placed in glass bottom culture dishes using Prolong Antifade medium (Invitrogen). Control experiments were performed to insure the specificity of primary antibodies (anti-β1 and anti-β4) by adding commercially available blocking peptide, which completely ablated staining. A Zeiss Axiovert inverted microscope and Axiovision 4.5 software package (Carl Zeiss Inc., Thornwood, NY) were used to acquire and deconvolve Z-stacks of fluorescent images and perform subsequent analysis.

To measure the intensity of specific BK β1 and β4 staining in each cell compartment, a deconvolution fast iterative algorithm was applied to sharpen the signal; the resulting images were used for quantification; each compartment of the cell (soma, dendrite, terminal) was outlined, and the average fluorescent density for each channel color was measured within these outlines; and mean density values were obtained from the corresponding histograms generated in Photoshop (Adobe Systems, Mountain View, CA). (The boundaries of each region were determined using the differential interference contrast image of the terminal overlapped onto the channel expression image.)

Statistics. Unless otherwise indicated, statistical significance between various groups was analyzed using Student's t test (Statistica, version 5.5; StatSoft, Tulsa, OK). All data are expressed as average ± S.E.M., and $p < 0.05$ was considered to be statistically significant.

Results

SON Dendrites Express Functional BK Channels. Previous studies reported the presence of BK channels in SON cell bodies and their nerve terminals in the neurohypophysis (Wang et al., 1992; Dopico et al., 1999). To extend the characterization of BK channels to include the dendritic compartment, we first confirmed that BK channels are present in the dendrite. Figure 1A shows a micrograph of a micropipette placed on a dendrite. We assessed basic electrophysiological properties including voltage sensitivity, calcium sensitivity, and conductance of dendritic channels in inside-out patches. Dendritic single channel currents were elicited by depolarizing the membrane from −80 to +80 mV in 20-mV increments while perfusing the intracellular surface with 5 μM free Ca^{2+}. For the channels shown in Fig. 1B, their open probability was very low, at potentials below −40 mV, and did not increase further above +40 mV. As such, they did not provide further useful information and are not shown. Thus, the activity of a two-channel patch recorded

between −40 and +40 mV is shown in Fig. 1B. At −40 mV, the channel displays a low open probability (NP_o = 0.097) but as the channel membrane is depolarized to +40 mV, the channels spend more time in the open state (NP_o = 0.92). The same patch was then clamped at −40 mV, and the systolic face was exposed to 1, 5, and 10 μm free Ca^{2+}. The channels are extremely calcium dependent, exhibiting low activity in 1 μm free Ca^{2+} (NP_o = 0.001), increasing activity to an NP_o of 0.169 in the presence of 5 μm free Ca^{2+} and reaching a nearly persistent open state in 10 μm free Ca^{2+} (NP_o = 0.79) (Fig. 1C). Figure 1D shows a plot of the current amplitude versus the membrane potential of a dendritic channel. The current-voltage relationship was well fitted with a linear regression (r = 0.99), yielding a slope conductance of 261 pS. In addition, current reversed at 0 mV in symmetric potassium conditions, $[K]_i = [K]_o$, indicating the channel is selective for potassium. These data are consistent with the known features of BK channels including potassium selectivity, large conductance (>180 pS), and sensitivity to intracellular calcium (McManus, 1991). To dependably compare the properties of BK channels in each of the three compartments, we repeated previously published characterizations of several BK channel parameters in the HNS cell body and nerve terminal in addition to those performed in the dendrite.

Conductance. In symmetric 135 mM K^+, with the intracellular face of inside-out patches exposed to 5 μM free Ca^{2+}, the conductance of dendritic BK channels was 247.0 ± 11.2 pS, n = 7. In contrast, under identical conditions, BK channels in nerve terminals had a conductance of 219 ± 4.84 pS, n = 4 (Fig. 2A), consistent with previously reported values (Pietrzykowski et al., 2004). Values obtained for cell body channels, 250.7 ± 9.4 pS (n = 9) in 5 μM free Ca^{2+} were very similar to dendritic channels. When exposed to 10 μM free Ca^{2+}, the conductance of somatic and dendritic channels was again similar, 248.3 ± 14.5 (n = 8) and 254 ± 7.03 (n = 6) pS, respectively (Fig. 2A). The conductance of BK channels from terminals in presence of 10 μM free Ca^{2+} was obtained from a previous publication (Dopico et al., 1996).

Calcium Dependence. Figure 2B shows the normalized NP_o of BK channels from SON terminals, soma, and dendrites as a function of membrane potential. The graph shows that the open probability of BK channels is steeply voltage dependent. The NP_o-voltage relationship could be well fitted with a Boltzmann equation. Consistent with previous data (Dopico et al., 1999), nerve terminal BK channels were less sensitive to 10 μM free Ca^{2+} than somatic channels ($V_{0.5}$ was −8.9 ± 3.5 mV, n = 7 in terminals and −30.6 ± 3.7 mV, n = 7 in cell body). Dendritic BK channels showed sensitivity to 10 μM free Ca^{2+} similar to somatic channels ($V_{0.5}$ was −22.5 ± 4.2 mV, n = 9) (Fig. 2B). In addition, the voltage necessary to produce an e-fold change in open probability (see *Materials and Methods*; reciprocal of the slope of the $\ln(P_o) - V$ relationship at low P_o) was similar for both somatic and dendritic SON channels (10.7 ± 1.5 and 11.6 ± 1.4, respectively). In the terminals, however, the voltage necessary to produce an e-fold change in open probability was 24 ± 2.8 mV. Taken together, these data suggest a relatively homogeneous BK channel profile in the somatic and dendritic compartments, which is markedly different from the channel population in the nerve terminal.

Because of the heavy dependence of BK channel open probability on calcium concentration, we determined whether the

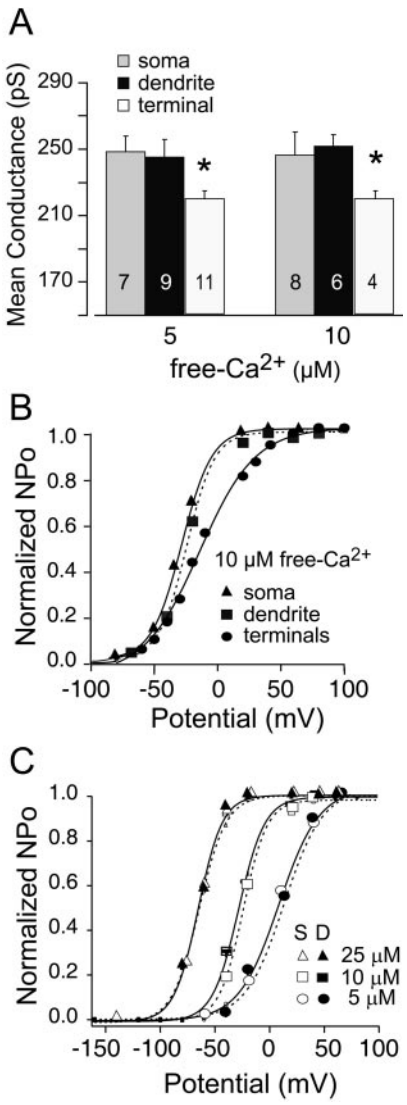

Fig. 2. Comparison of the conductance and calcium dependence of somatic, dendritic, and nerve terminal BK channels. A, mean conductance of somatic, dendritic, and nerve terminal channels measured in the presence of 5 and 10 μM free Ca^{2+}. B, normalized NP_o-voltage relationship of SON somatic and dendritic channels compared with SON nerve terminal channels in 10 μM free Ca^{2+} (S.E.M. not shown to reduce clutter). Somatic, dendritic, and nerve terminal are shown as triangles, squares, and circles, respectively. C, plots of normalized mean NP_o as a function of voltage at different $[Ca^{2+}]i$; circles, 5 μM; squares, 10 μM; triangles, 25 μM. Open and filled symbols, soma and dendrite, respectively. The NP_o-V relationship, fitted with a Boltzmann equation, is shifted along the voltage axis to more negative potentials as $[Ca^{2+}]_i$ increases.

similarity between open probability of dendritic and somatic BK channels extended across a range of calcium concentrations. As shown in Fig. 2C, the open probability of BK channels is steeply calcium- and voltage-dependent because as the calcium concentration is decreased, the membrane must be depolarized more to produce a similar open probability (seen as a shift to the right). The graph shows the similarity between cell body and dendritic channels obtained from an examination of channel activity in 5, 10, and 25 μM free Ca^{2+}. The potential at which half of the BK channels were open ($V_{0.5}$) in 25 μM free Ca^{2+} was −65.6 ± 2.9 (n = 12) and −68.7 ± 3.3 (n = 10) mV in the soma and dendrites, respectively. In 10 μM free Ca^{2+}, $V_{0.5}$ was −30.6 ± 3.7 (n = 7) and

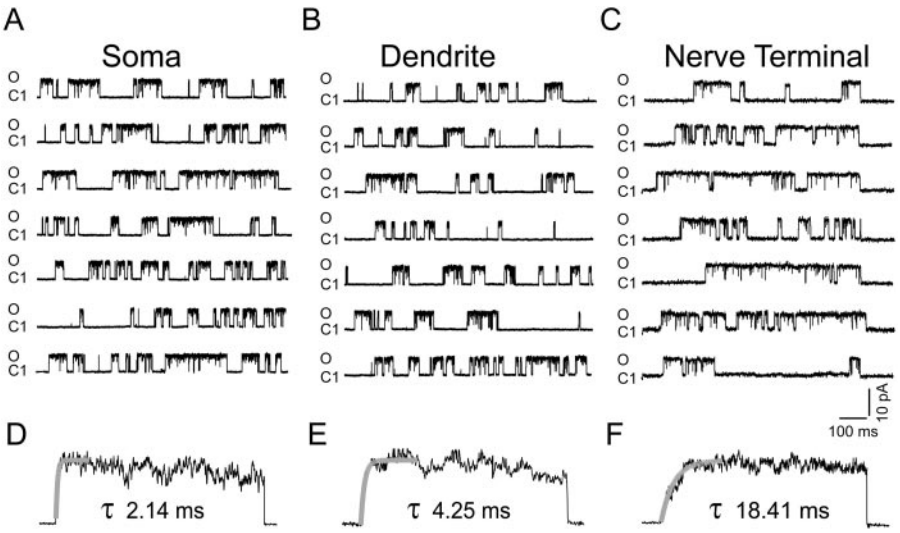

Fig. 3. Gating properties of nerve terminal channels differ from that of somatic and dendritic channels. A series of seven consecutive BK traces evoked by depolarizing: A, somatic; B, dendritic; or C, nerve terminal membrane patches from 0 to +40 mV. Channel activity was recorded in 10 μM free Ca^{2+} in an inside-out patch. C and O1, closed and open states, respectively. D to F, aggregate of 100 consecutive individual single channel traces recorded from one BK channel in a membrane patch excised from soma, dendrite, and terminal compartments, respectively. In all cases, BK current activation was best fit with a single exponential whose value (τ) is indicated below the aggregate traces.

−22.5 ± 4.2 (n = 9) mV in the soma and dendrites, respectively. Finally, in 5 μM free Ca^{2+}, $V_{0.5}$ was 8.5 ± 3.7 (n = 8) and 13.1 ± 1.9 (n = 11) mV in the soma and dendrites, respectively (Fig. 2C). In summary, we found that the NP_o-voltage relationship of dendritic and somatic channels is very similar across a range of calcium concentrations.

Activation Kinetics of BK Channels in Cell Bodies and Dendrites versus Nerve Terminal Compartments. Although whole-cell patch clamp is generally used to study kinetic properties, such as activation, we could not use this approach because it would not have enabled us to independently examine BK channel properties in each region of the cell. Moreover, single channel records assure that our data are not contaminated with non-BK currents. Therefore, to study channel kinetics, we compiled a cumulative current trace from the summation of 100 repetitively evoked single channel sweeps. The resulting current trace resembles the classical macroscopic current recorded in whole-cell patch-clamp configuration. The membrane of an inside-out patch was stepped from a holding potential of 0 to +40 mV in the presence of 10 μM free Ca^{2+}. A typical example showing seven of 100 consecutive traces from somatic, dendritic, and nerve terminal channels is shown in Fig. 3, A to C. An example of the compiled macroscopic current from the soma, dendrite, and nerve terminal is shown in Fig. 3, D to F. In both the cell body and dendrite, currents were well fitted with a single exponential (τ was 3.4 ± 1.18 ms (n = 6) in the soma and 5.7 ± 2.34 ms (n = 7) in the dendrites), indicating that these channels have relatively fast activation kinetics. In contrast, nerve terminal channels display much slower gating kinetics [τ = 22.7 ± 4.19 ms (n = 3)].

Ethanol Selectively Potentiates Nerve Terminal but Not Somatic and Dendritic BK Channels. The BK channel is a well studied target of ethanol action, and although BK channels in HNS terminals are highly sensitive to ethanol, exhibiting increased channel activity within a few minutes, BK channels in the cell body of these neurons are insensitive to the drug (Dopico et al., 1999). Here, we examine the sensitivity of dendritic BK channels (Fig. 4). The ethanol sensitivity of BK channels in proximal dendrites (20–40 μM from the soma) was examined in inside-out patches in the presence of 5 μm free Ca^{2+} at a membrane potential of −40 mV. The ethanol concentrations chosen were within a clinically relevant range from 20 mM ethanol (EtOH) (resulting in intoxication) to 100 mM EtOH (lethal in naive subjects) (Madeira et al., 1993; Ruela et al., 1994). In

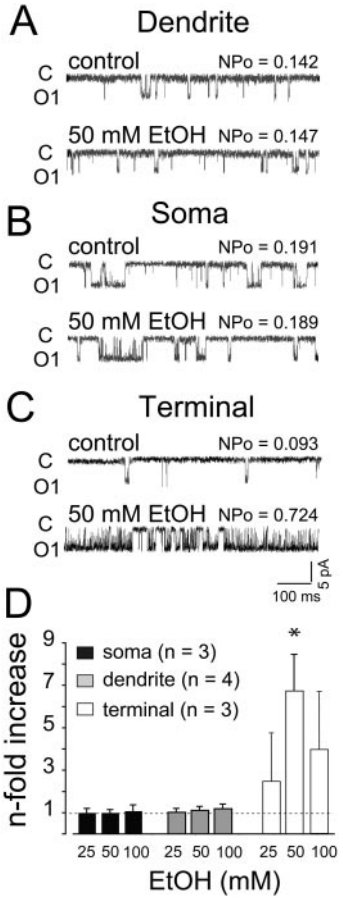

Fig. 4. EtOH exposure increases BK channel activity in the nerve terminal but not in soma or dendrite. Traces of BK channel activity before and during exposure to 50 mM EtOH (V_h = −40 mV, 5 μM free Ca^{2+}) in: A, dendrite; B, soma; or C, nerve terminal patches. C and O1, closed and open state, respectively. D, plot of the effects of various EtOH concentrations on somatic, dendritic, and terminal BK channels. The numbers within the bars represent the number of patches tested. *, statistical significance of $p < 0.01$. Data showing the response to 25 and 100 mM EtOH of BK channels in terminals are from a previous publication (Dopico et al., 1996).

the dendrite, the baseline probability of BK channel opening is low ($NP_o = 0.142$) at −40 mV. During application of 50 mM EtOH, channel activity was recorded every 60 s for 10 min. Throughout the entire period of EtOH exposure, channel activity remained unchanged (99 ± 14% of control; $n = 4$) (Fig. 4, A and D). Similar results were obtained with 25 and 100 mM ethanol (99 ± 19% of control values, $n = 4$, and 107 ± 29% of control, $n = 4$, respectively) (Fig. 4D). Twenty-five, 50, or 100 mM EtOH did not potentiate somatic channels [102 ± 17% ($n = 3$), 111 ± 16% of control ($n = 3$), and 118 ± 21%, respectively] (Fig. 4, B and D), further supporting the notion that cell body and dendrite channels are similar. In contrast, EtOH greatly potentiated the activity of channels in dissociated nerve terminals in a dose-dependent fashion. The peak effect was observed with 50 mM EtOH (673 ± 171%, $n = 3$), consistent with previous data (Dopico et al., 1996; Pietrzykowski et al., 2004) (Fig. 4, C and D). The response of BK channels from terminals to 25 and 100 mM EtOH are reproduced from a previous publication (Dopico et al., 1996). We did not observe any channels that were inhibited by the drug.

Expression of BK β Subunits in the Three Compartments of the HNS. One possible explanation for these findings is a selective regional distribution of the auxiliary β1 subunit to the somatic and dendritic compartments and β4 subunit to the terminal compartment. Iberiotoxin provides a useful pharmacological tool to distinguish αβ4 from α or αβ1 channels. Expression studies have shown that α or αβ1 BK channels are blocked by nanomolar concentrations of the scorpion toxins, iberiotoxin and charybdotoxin, whereas the presence of the β4 subunit renders BK channels insensitive to these toxins (Hanner et al., 1998; Lippiat et al., 2003). To assess iberiotoxin sensitivity, outside-out patches held at +40 mV were perfused with 50 nM iberiotoxin (IbTX) in 5 μM free Ca^{2+}. IbTX strongly inhibited both dendritic (NP_o decreased 81 and 75%, $n = 2$) and somatic (NP_o decreased 83% and 71%, $n = 2$) (data not shown) channels. IbTX blockade of somatic channels is consistent with previously reported findings (Dopico et al., 1999). In contrast, IbTX had no effect on BK channels in the terminal (NP_o changed 0.5 and 0.2%, $n = 2$) (data not shown), consistent with previously reported findings that terminal channels are insensitive to blockade by the scorpion toxin, charybdotoxin (Wang et al., 1992). These data support the notion that αβ4 channels are present in the nerve terminal and absent in both the cell body and dendrite. However, because both α and αβ1 channels are iberiotoxin sensitive, we were unable to use this pharmacological tool to establish the selective presence of the αβ1 channel in the cell body and dendrite.

To determine whether β1 subunits were present in the somatic and dendritic compartments, we immunolabeled coronal sections of rat SON tissue with antibodies to the β1 or β4 subunit and AVP neurophysin, a known marker for SON magnocellular neurons (Fig. 5). The punctate anti-β1 staining indicates that BK β1 channel clusters are located throughout the cell body and in both proximal and distal dendrites (arrowheads, Fig. 5C). In contrast, surrounding regions of the brain had very low to nonexistent β1 staining, suggesting this antibody is highly specific (Fig. 5A). In contrast to the robust β1 staining, β4 staining in SON cell bodies and dendrites was extremely faint (Fig. 5B).

To confirm the distribution of β4 subunits to the nerve terminal, we immunolabeled dissociated terminals with antibodies to the β1 or β4 subunit, AVP and OXT. We then selected terminals ranging in size from 5 to 10 μm for image analysis. These terminals, when labeled with the same concentrations used to stain the SON, displayed distinct punctate β4 clusters (Fig. 6B, left), whereas the β1 subunit was barely detectable (Fig. 6A, left). Antibody specificity was appropriately controlled for by either omitting the primary antibody or preabsorbing with blocking peptide. In addition, both the anti-β1 and anti-β4 antibodies have been show to be immunoreactive in wild-type mice, with no specific staining in β1- and β4- deficient mice, respectively (Grimm et al., 2007; Piwonska et al., 2008).

We quantified the intensity of the immunofluorescence signal for β1 and β4 antibodies in the dendrites, soma, and terminals (Fig. 6C). For β1 subunits, the optical density was much greater in the soma (25.83 ± 2.15; $n = 3$) and the dendrites (27.93 ± 0.07) compared with the terminals (1.97 ± 1.52). It is interesting that the ratio was reversed for β4 expression. Thus, in the soma and dendrites, the mean optical density of β4 was 6.75 ± 0.88 and 0.35 ± 0.18, respectively, whereas in the terminals, the value was much higher (33.93 ± 3.1).

Discussion

The data presented in this article demonstrate: 1) the expression of functional BK channels on the membranes of dendrites, somata, and nerve terminals of hypothalamic magnocellular neurons; 2) selective expression of β1-contain-

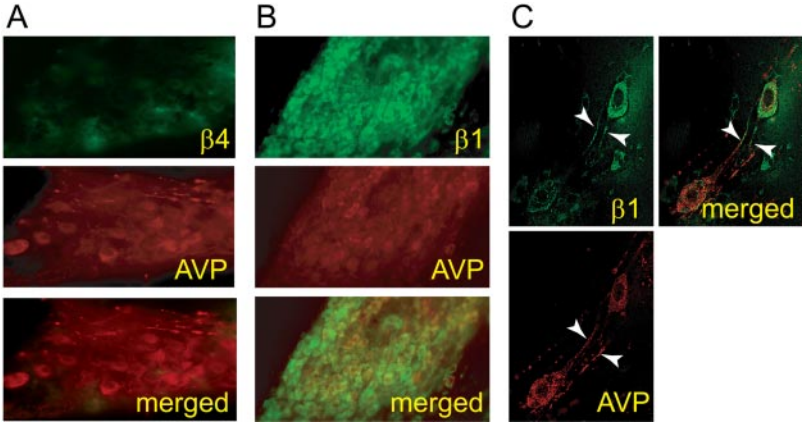

Fig. 5. Punctate clusters of BK β1 subunits are located in the cell body and peripheral processes of magnocellular neurons. Magnification, 20×, of a section from fixed adult rat brain immunolabeled with: A, anti-β4-conjugated followed by mouse secondary Alexa 488-conjugated antibody; or B, anti-β1- and Alexa 488-conjugated antibody. C, magnification, 63×, of two neurons labeled with anti-β1- and Alexa 488-conjugated antibody. The sections in A to C are counterstained with anti-AVP neurophysin- and Alexa 594-conjugated antibody. Arrowheads, stained dendrites.

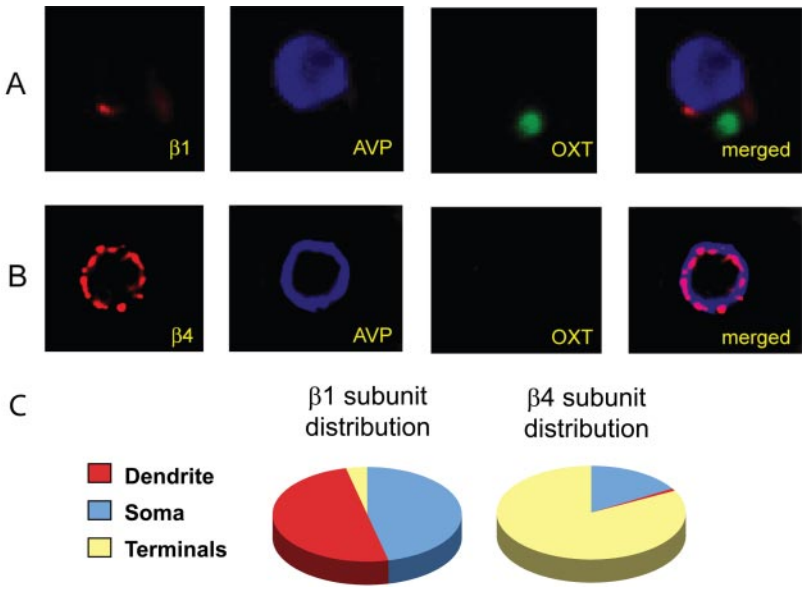

Fig. 6. BK β4 subunits in HNS nerve terminals. Single HNS nerve terminals magnified at 63× immunolabeled with: A, anti-β1-conjugated and mouse secondary Alexa 594-conjugated antibody; or B, anti-β4- and mouse secondary Alexa 594-conjugated antibody. Nerve terminals are counterstained with: 1, anti-AVP neurophysin- and rabbit secondary Alexa 350-conjugated antibody; and 2, anti-OXT-conjugated and rabbit secondary Alexa 488-conjugated antibody. C, pie charts of the optical density of β1 (left chart) and β4 (right chart) immunofluorescence in the dendrite (red), soma (blue), and terminal (yellow) compartments of SON neurons.

ing BK channels in cell body and dendrite; 3) selective expression of β4-containing BK channels in the nerve terminal; and 4) ethanol potentiation of nerve terminal β4-containing BK channels but not somatic and dendritic β1-containing BK channels.

Regional Distribution of BK β Subunits in Three Compartments of a Single HNS Neuron. This study has examined the characteristics of BK channel subtypes in each of the three compartments of a neuron (dendrite, cell body, and nerve terminal) utilizing the unique advantages of the hypothalamic-neurohypophysial system. In doing so, we discovered that in these neurons, BK channels were similar in the somatic and dendritic compartments. In contrast, we observed markedly different BK channels in the nerve terminal. Properties of both cell body and dendritic BK channels include: 1) increased calcium sensitivity compared with nerve terminal channels, manifested as a shift in the voltage required to activate the channel to more hyperpolarized potentials; 2) fast activation kinetics; 3) insensitivity to ethanol; and 4) blockade by iberiotoxin. Properties of exogenously expressed αβ1 channels (Jiang et al., 1999; Feinberg-Zadek and Treistman, 2007) match the biophysical and pharmacological properties of HNS somatic and dendritic channels, suggesting the presence of β1 in this compartment.

Nerve terminal channels, on the other hand, display the following properties: 1) decreased calcium sensitivity compared with somatic and dendritic channels, manifested as a shift in the voltage required to activate the channel to more depolarized potentials; 2) slow activation kinetics; 3) sensitivity to ethanol; and 4) insensitivity to iberiotoxin blockade. Consistent with exogenous αβ4 expression studies (Behrens et al., 2000; Feinberg-Zadek and Treistman, 2007), these biophysical and pharmacological properties suggest that HNS nerve terminal channels contain the β4 subunit. Immunostaining with antibodies to either the β1 or β4 subunit confirmed the regional distribution of BK αβ1 channels in the somatic and dendritic compartments and BK αβ4 channels in nerve terminals.

Regional subcellular distribution of channel subtypes is not limited to BK channels but also has been reported for other channel types. For example, K_v3.1 voltage-gated potassium channel splice variants are differentially distributed in the reticular thalamus, where the K_v3.1b isoform is localized to the soma and proximal dendrites, whereas the K_v3.1a isoform is selectively restricted to axonal processes (Ozaita et al., 2002). There are also reports that T-type calcium channel isoforms selectively distribute to the soma or dendrite dependent upon neuronal type (McKay et al., 2006). Furthermore, HCN channels display subunit-specific subcellular distribution patterns in the hippocampus dependent upon stage of development (Brewster et al., 2007). These illustrative examples emphasize that the selective distribution of ion channels within a neuron plays an important role in cell polarity and neuronal specialization.

A number of mechanisms may underlie the selective distribution of ion channels within neurons. Several mRNAs, such as arginine vasopressin and calcium calmodulin-dependent protein kinase II, contain a dendritic localizer sequence, which targets the mRNA to the dendritic compartment (Blichenberg et al., 2001; Mohr and Richter, 2004). An additional mechanism for controlling localization is through postsynaptic density 95/disc-large/zona occludens-containing anchoring proteins that target G-protein-gated K^+ channels (Kir3.2c) to the postsynaptic density in dopaminergic neurons of the substantia nigra (Kurachi and Ishii, 2004). Lastly, β subunits of channels also have been proposed to play a role in localization. For instance, association of the auxiliary β subunit with the calcium channel α1 subunit results in increased membrane localization (Bichet et al., 2000).

Compartment-Specific Ethanol Effects on BK Channels Are Determined by Regional Specificity of β Subunit. A strong correlation between BK β subunit identity and ethanol sensitivity has been shown in human embryonic kidney 293 expression studies (Feinberg-Zadek and Treistman, 2007) and freshly dissociated rat nucleus accumbens neurons (Martin et al., 2004). In medium spiny neurons, the effects of EtOH on BK channels are regionally specific, similar to the HNS. It is interesting that in contrast to the HNS, BK channels in the cell bodies of medium spiny neurons are sensitive to EtOH, whereas those in dendrites are insensitive to the drug. In these neurons, this dichotomy correlates with the differential distribution of β1 and β4 subunits to the

dendrite and soma, respectively. Likewise, we suggest that the observed differences in ethanol sensitivity among HNS somatic, dendritic, and nerve terminal channels reflect a differential distribution of β1 and β4 subunits.

A link between subunit composition and ethanol sensitivity also has been reported for other ion channels. For example, the effects of ethanol on P2X receptors are dependent upon receptor subtype, with P2X3 receptors potentiated and P2X4 receptors inhibited by EtOH (Davies et al., 2005). NMDA receptor NR2 subunits and NR1 splice variants also are thought to confer differential sensitivity to EtOH-induced inhibition of NMDA currents (Chu et al., 1995). Furthermore, various AMPA receptor subtypes are also differentially sensitive to ethanol (Akinshola et al., 2003).

Although we propose that regional ethanol sensitivity within magnocellular neurons in the HNS is conferred through subunit composition, several other factors may also play a role. These factors include variations in BK α subunit splice variants, regional differences in lipid bilayer composition, and post-translational modification. For example, expression studies in human embryonic kidney 293 cells indicate that certain BK α isoforms such as stress-regulated exon are alcohol insensitive (Pietrzykowski et al., 2008). In addition, bilayer studies have shown that modulation of the lipid environment can alter BK channel sensitivity to ethanol (Crowley et al., 2005). Lastly, post-translational modifications, including phosphorylation status of BK channels, also have been shown to alter ethanol sensitivity (Liu et al., 2006).

Functional Implications. The selective regional distribution of alcohol-sensitive and -insensitive channels in the HNS has interesting implications for synaptic integration. The SON receives excitatory glutamatergic inputs from areas such as the amygdala, the suprachiasmatic nucleus, and the lamina terminalis (Csáki et al., 2002). In addition, the SON receives inhibitory GABAergic inputs from areas such as the nucleus accumbens, a region known to play a role in addiction (Shibuki, 1984). Both excitatory glutamatergic and inhibitory GABAergic inputs establish synaptic contact primarily on the dendrites of the SON, which generally comprise approximately 80% of the neuron's surface area. The selective distribution of dendritic channels insensitive to acute EtOH may suggest that the effects of alcohol on HNS neurons mediated through BK channels have little direct impact on the integration of dendritic electrical activity. Instead, the selective distribution of ethanol-sensitive BK channels to the nerve terminal compartment suggests that the effect of alcohol on HNS neurons mediated through BK channels is largely confined to the nerve terminal.

In addition to the role that nerve terminal BK channels play in mediating HNS responses to ethanol, somatic and dendritic BK channels also may contribute indirectly to ethanol effects, despite their apparent insensitivity to the drug. This possibility exists because BK channels can form heteromultimeric complexes with both voltage-gated calcium channels and NMDA receptors (Marrion and Tavalin, 1998; Isaacson and Murphy, 2001). Ethanol inhibits voltage-gated calcium channels and NMDA receptors, thereby lowering intracellular calcium levels (Widmer et al., 1998). As a result, ethanol-induced changes in intracellular dendritic calcium levels may be transduced by associated calcium-activated BK channels, ultimately influencing input and output patterns of HNS neurons. Thus, the presence of BK channels in somatic, dendritic, and nerve terminal compartments of HNS neurons, and their corresponding differential sensitivity to ethanol, may play an important role in the response to ethanol.

Peptide Hormone Release. In the HNS, all three cellular compartments (dendrite, soma, and nerve terminal) secrete the peptides OXT and AVP. The dendrites and cell bodies of magnocellular neurons release OXT and AVP centrally into the brain, whereas nerve terminals release OXT and AVP peripherally into systemic circulation. It is of particular interest that, although both dendrites and nerve terminals secrete AVP and OXT, release from these two compartments can occur independently and is differently regulated (for review, see Ludwig and Leng, 2006). In terminals, peptide release is regulated in an activity-dependent manner when membrane depolarization elicits calcium entry through voltage-gated calcium channels. Dendritic release, on the other hand, is triggered not only by depolarization-induced calcium entry but also by the release of calcium from intracellular stores in response to the binding of AVP or OXT to its corresponding autoreceptor. Our study shows that these two compartments, the nerve terminal and dendrite, have distinctly different BK channels with varying calcium sensitivities, which may contribute to differences in the regulation of peptide release.

Acknowledgments

We thank Andy Wilson, Sonia Ortiz-Miranda, and José Lemos for technical and critical advice.

References

Akinshola BE, Yasuda RP, Peoples RW, and Taylor RE (2003) Ethanol sensitivity of recombinant homomeric and heteromeric AMPA receptor subunits expressed in *Xenopus* oocytes. *Alcohol Clin Exp Res* **27:**1876–1883.

Behrens R, Nolting A, Reimann F, Schwarz M, Waldschütz R, and Pongs O (2000) hKCNMB3 and hKCNMB4, cloning and characterization of two members of the large-conductance calcium-activated potassium channel beta subunit family. *FEBS Lett* **474:**99–106.

Benhassine N and Berger T (2005) Homogeneous distribution of large-conductance calcium-dependent potassium channels on soma and apical dendrite of rat neocortical layer 5 pyramidal neurons. *Eur J Neurosci* **21:**914–926.

Bichet D, Cornet V, Geib S, Carlier E, Volsen S, Hoshi T, Mori Y, and De Waard M (2000) The I-II loop of the Ca^{2+} channel alpha1 subunit contains an endoplasmic reticulum retention signal antagonized by the beta subunit. *Neuron* **25:**177–190.

Blichenberg A, Rehbein M, Müller R, Garner CC, Richter D, and Kindler S (2001) Identification of a cis-acting dendritic targeting element in the mRNA encoding the alpha subunit of Ca^{2+}/calmodulin-dependent protein kinase II. *Eur J Neurosci* **13:**1881–1888.

Brenner R, Jegla TJ, Wickenden A, Liu Y, and Aldrich RW (2000) Cloning and functional characterization of novel large conductance calcium-activated potassium channel beta subunits, hKCNMB3 and hKCNMB4. *J Biol Chem* **275:**6453–6461.

Brewster AL, Chen Y, Bender RA, Yeh A, Shigemoto R, and Baram TZ (2007) Quantitative analysis and subcellular distribution of mRNA and protein expression of the hyperpolarization-activated cyclic nucleotide-gated channels throughout development in rat hippocampus. *Cereb Cortex* **17:**702–712.

Chu B, Anantharam V, and Treistman SN (1995) Ethanol inhibition of recombinant heteromeric NMDA channels in the presence and absence of modulators. *J Neurochem* **65:**140–148.

Crowley JJ, Treistman SN, and Dopico AM (2005) Distinct structural features of phospholipids differentially determine ethanol sensitivity and basal function of BK channels. *Mol Pharmacol* **68:**4–10.

Csáki A, Kocsis K, Kiss J, and Halász B (2002) Localization of putative glutamatergic/aspartatergic neurons projecting to the supraoptic nucleus area of the rat hypothalamus. *Eur J Neurosci* **16:**55–68.

Davies DL, Kochegarov AA, Kuo ST, Kulkarni AA, Woodward JJ, King BF, and Alkana RL (2005) Ethanol differentially affects ATP-gated P2X(3) and P2X(4) receptor subtypes expressed in *Xenopus* oocytes. *Neuropharmacology* **49:**243–253.

Dopico AM, Lemos JR, and Treistman SN (1996) Ethanol increases the activity of large conductance, $Ca^{(2+)}$-activated K^+ channels in isolated neurohypophysial terminals. *Mol Pharmacol* **49:**40–48.

Dopico AM, Widmer H, Wang G, Lemos JR, and Treistman SN (1999) Rat supraoptic magnocellular neurones show distinct large conductance, Ca^{2+}-activated K^+ channel subtypes in cell bodies versus nerve endings. *J Physiol* **519:**101–114.

Dworetzky SI, Boissard CG, Lum-Ragan JT, McKay MC, Post-Munson DJ, Trojnacki

JT, Chang CP, and Gribkoff VK (1996) Phenotypic alteration of a human BK (hSlo) channel by hSlobeta subunit coexpression: changes in blocker sensitivity, activation/relaxation and inactivation kinetics, and protein kinase A modulation. *J Neurosci* **16:**4543–4550.

Feinberg-Zadek PL and Treistman SN (2007) Beta-subunits are important modulators of the acute response to alcohol in human BK channels. *Alcohol Clin Exp Res* **31:**737–744.

Grimm PR, Foutz RM, Brenner R, and Sansom SC (2007) Identification and localization of BK-beta subunits in the distal nephron of the mouse kidney. *Am J Physiol Renal Physiol* **293:**F350–F359.

Hanner M, Vianna-Jorge R, Kamassah A, Schmalhofer WA, Knaus HG, Kaczorowski GJ, and Garcia ML (1998) The beta subunit of the high conductance calcium-activated potassium channel: identification of residues involved in charybdotoxin binding. *J Biol Chem* **273:**16289–16296.

Isaacson JS and Murphy GJ (2001) Glutamate-mediated extrasynaptic inhibition: direct coupling of NMDA receptors to $Ca^{(2+)}$-activated K^+ channels. *Neuron* **31:** 1027–1034.

Jiang Z, Wallner M, Meera P, and Toro L (1999) Human and rodent MaxiK channel beta-subunit genes: cloning and characterization. *Genomics* **55:**57–67.

Kurachi Y and Ishii M (2004) Cell signal control of the G protein-gated potassium channel and its subcellular localization. *J Physiol* **554:**285–294.

Lippiat JD, Standen NB, Harrow ID, Phillips SC, and Davies NW (2003) Properties of BK(Ca) channels formed by bicistronic expression of hSloalpha and beta1–4 subunits in HEK293 cells. *J Membr Biol* **192:**141–148.

Liu J, Asuncion-Chin M, Liu P, and Dopico AM (2006) CaM kinase II phosphorylation of slo Thr107 regulates activity and ethanol responses of BK channels. *Nat Neurosci* **9:**41–49.

Ludwig M and Leng G (2006) Dendritic peptide release and peptide-dependent behaviours. *Nat Rev Neurosci* **7:**126–136.

Madeira MD, Sousa N, Lieberman AR, and Paula-Barbosa MM (1993) Effects of chronic alcohol consumption and of dehydration on the supraoptic nucleus of adult male and female rats. *Neuroscience* **56:**657–672.

Marrion NV and Tavalin SJ (1998) Selective activation of Ca^{2+}-activated K^+ channels by co-localized Ca^{2+} channels in hippocampal neurons. *Nature* **395**:900–905.

Martin G, Puig S, Pietrzykowski A, Zadek P, Emery P, and Treistman S (2004) Somatic localization of a specific large-conductance calcium-activated potassium channel subtype controls compartmentalized ethanol sensitivity in the nucleus accumbens. *J Neurosci* **24:**6563–6572.

McKay BE, McRory JE, Molineux ML, Hamid J, Snutch TP, Zamponi GW, and Turner RW (2006) Ca(V)3 T-type calcium channel isoforms differentially distribute to somatic and dendritic compartments in rat central neurons. *Eur J Neurosci* **24:**2581–2594.

McManus OB (1991) Calcium-activated potassium channels: regulation by calcium. *J Bioenerg Biomembr* **23:**537–560.

Mohr E and Richter D (2004) Subcellular vasopressin mRNA trafficking and local translation in dendrites. *J Neuroendocrinol* **16:**333–339.

Ozaita A, Martone ME, Ellisman MH, and Rudy B (2002) Differential subcellular localization of the two alternatively spliced isoforms of the Kv3.1 potassium channel subunit in brain. *J Neurophysiol* **88:**394–408.

Pietrzykowski AZ, Friesen RM, Martin GE, Puig SI, Nowak CL, Wynne PM, Siegelmann HT, and Treistman SN (2008) Posttranscriptional regulation of BK channel splice variant stability by miR-9 underlies neuroadaptation to alcohol. *Neuron* **59:**274–287.

Pietrzykowski AZ, Martin GE, Puig SI, Knott TK, Lemos JR, and Treistman SN (2004) Alcohol tolerance in large-conductance, calcium-activated potassium channels of CNS terminals is intrinsic and includes two components: decreased ethanol potentiation and decreased channel density. *J Neurosci* **24:**8322–8332.

Piwonska M, Wilczek E, Szewczyk A, and Wilczynski GM (2008) Differential distribution of $Ca^{(2+)}$-activated potassium channel beta4 subunit in rat brain: immunolocalization in neuronal mitochondria. *Neuroscience* **153:**446–460.

Ruela C, Sousa N, Madeira MD, and Paula-Barbosa MM (1994) Stereological study of the ultrastructural changes induced by chronic alcohol consumption and dehydration in the supraoptic nucleus of the rat hypothalamus. *J Neurocytol* **23:**410–421.

Sailer CA, Kaufmann WA, Kogler M, Chen L, Sausbier U, Ottersen OP, Ruth P, Shipston MJ, and Knaus HG (2006) Immunolocalization of BK channels in hippocampal pyramidal neurons. *Eur J Neurosci* **24:**442–454.

Shibuki K (1984) Supraoptic neurosecretory cells: synaptic inputs from the nucleus accumbens in the rat. *Exp Brain Res* **53:**341–348.

Wallner M, Meera P, and Toro L (1996) Determinant for beta-subunit regulation in high-conductance voltage-activated and $Ca^{(2+)}$-sensitive K^+ channels: an additional transmembrane region at the N terminus. *Proc Natl Acad Sci U S A* **93:** 14922–14927.

Wang G, Thorn P, and Lemos JR (1992) A novel large-conductance $Ca^{(2+)}$-activated potassium channel and current in nerve terminals of the rat neurohypophysis. *J Physiol* **457:**47–74.

Widmer H, Lemos JR, and Treistman SN (1998) Ethanol reduces the duration of single evoked spikes by a selective inhibition of voltage-gated calcium currents in acutely dissociated supraoptic neurons of the rat. *J Neuroendocrinol* **10:**399–406.

Address correspondence to: Dr. Steven N. Treistman, Institute of Neurobiology, University of Puerto Rico, 201 Blvd del Valle, San Juan, Puerto Rico 00901. E-mail: steven.treistman@upr.edu